^{169}Yb-DTPA DISTRIBUTION AND DOSIMETRY IN CISTERNOGRAPHY

Richard L. Morin and Valerie A. Brookeman

Veterans Administration Hospital and University of Florida College of Medicine, Gainesville, Florida

Following intrathecal administration of 1 mCi ^{169}Yb-DTPA to nine patients, spinal counts were obtained from 2 to 48 hr with a gamma camera/computer system. Utilizing computer outputs, the length of the spine was divided into six equal segments approximately 2 in. wide. The counts in each segment at each time were corrected for the surrounding blood background and converted to the percent of administered activity by reference to a standard. The cumulated activity in each segment was determined by graphic integration of mean activity–time curves. Absorbed radiation doses were computed for cylindrical geometry utilizing appropriate reduction coefficients for the dose contribution from electrons. Maximum doses to the surfaces of the cord and nerve roots are 31 ± 18 and 46 ± 20 rads, respectively, for 1 mCi ^{169}Yb-DTPA administered. By a depth of 0.01 cm, the thickness of the pia, these doses decrease to the average values of 5 ± 3 and 8 ± 3 rads, respectively. Surface and average doses to the cord and nerve roots from intrathecal administration of 400 μCi ^{169}Yb-DTPA are about the same as those from 100 μCi ^{131}I-IHSA.

The radiopharmaceutical most recently available for routine use in cisternography is ^{169}Yb-diethylenetriaminepentaacetic acid (^{169}Yb-DTPA). Although ^{169}Yb has a physical half-life of 32 days, the chelated compound can be administered in millicurie quantities due to its rapid clearance from the vascular pool (*1–5*). Ytterbium-169-DTPA has a molecular weight of 603, which is acceptable for cisternography (*3,4,6*), and because of the high photon yield of 0.55 photons per disintegration for the 177- and 198-keV emissions (*2,7*) and long physical half-life, satisfactory images can be obtained as late as 108 hr following injection (*4*). This investigation was undertaken to examine the distribution and clearance of ^{169}Yb-DTPA during cisternography for the purpose of calculating absorbed radiation doses to the spinal cord and nerve roots.

MATERIALS AND METHODS

Sixteen patients, who were referred to the Nuclear Medicine Department, VA Hospital, Gainesville, Florida, for routine cisternography were studied. However, satisfactory data which could be utilized for dosimetry purposes were obtained from only nine patients. These were classified into clinical categories (Table 1) on the basis of cisternographic findings, x-ray findings (pneumoencephalogram), and review of each patient's chart. No normal individuals were studied. All patients studied exhibited delayed flow.

All patients were injected on the ward in the lateral decubitus position. A 20-gage spinal needle was inserted in the region of the fourth lumbar vertebra and ^{169}Yb-DTPA (3M Co.), diluted with normal saline to approximately 1 ml total volume, was slowly administered without barbotage. Unless it was absolutely clinically necessary, cerebrospinal fluid (CSF) samples were not taken and pressure was not measured.

Patient counting was performed using a gamma camera (Searle Radiographics Pho/Gamma HP)—computer (Digital Equipment Corp.—PDP-8/I) sys-

Received Dec. 14, 1973; revision accepted April 11, 1974.

For reprints contact: Valerie A. Brookeman, University of Florida College of Medicine, Dept. of Radiology, Box 219, Gainesville, Fla. 32610.

TABLE 1. PATIENT CLASSIFICATION

Patient No.	Cisternographic findings	Clinical category
02*	Slightly delayed flow	Cerebral atrophy
03	Delayed flow over convexities	Normal pressure hydrocephalus
06	Delayed flow over convexities	Cerebral atrophy
07†	Delayed flow over convexities with transient ventricular filling	Normal pressure hydrocephalus
08	Obstruction to flow	Porencephalic cyst
10	Delayed flow over convexities	Cerebral atrophy
12	Delayed flow over convexities	Partial obstruction to CSF flow
14	Slightly delayed flow	Cerebral atrophy
15†	Delayed flow over convexities with transient ventricular filling	Normal pressure hydrocephalus
16†	Delayed flow over convexities	Normal pressure hydrocephalus

* Blood data only.
† Spinal segment data only.

tem (*8*), which represented the camera field of view as a 50 × 50 matrix. A 4000-hole straight-bore collimator was utilized for all patient counting, and all computer data were stored on DEC tape for later analysis. Computer outputs were obtained with a line printer.

Spinal data collection. All counting was performed with the patient in prone position. On each patient, the injection site was delineated with a ^{169}Yb marker and the lengths from the base of the skull to the tip of the coccyx and from the base of the skull to the injection site were measured. In order to duplicate patient positioning for later counting, fuchsin carbol stain solution (Curtin Scientific Co.) was used to mark the patient's back before taking initial counts. Two vinyl sheets impregnated with lead were placed 10 in. apart across the patient's back to define the spinal segment to be recorded. Head images were obtained first followed by the spinal images which were obtained sequentially, moving down the spine in the caudal direction. Counts were recorded with the camera/computer system for 3 min/image at approximately 2, 6, 9, 24, and 48 hr following injection. This time schedule was adopted in order to coincide with the routine procedure for cisternography in our laboratory.

Counting standards. A spinal needle (20 gage) and syringe (1 ml) identical to that used for patient injection were filled with a known amount of ^{169}Yb-DTPA for use as a standard. Following patient injection, the syringe and spinal needle used were filled with water to a volume equal to that of the standard (0.9 ml) and both this and the standard were counted in identical fashion with the gamma camera. Thus the activity remaining in the syringe and needle was determined and, hence, the injected activity. The amount of ^{169}Yb-DTPA administered to each patient ranged from 0.87 to 1.15 mCi (mean, 0.93 mCi).

The activity in each spinal segment was determined by comparison with a spinal segment standard consisting of a Lucite cylinder, 1.5 in. (i.d.) and 10 in. long, filled with a known amount of ^{169}Yb-DTPA in 290 ml of water. Each day patients were counted, the spinal segment standard was also counted for 3 min with identical gamma camera settings and pressed wood (3.75 cm) between the standard and the collimator face. This method of standard counting has been shown (*9*) to be an accurate representation of spinal CSF activity.

A counting standard for blood samples was prepared by pipetting 1 ml (equivalent volume) ^{169}Yb-DTPA into a disposable counting tube identical to those used for samples.

Spinal data analysis. Computer data were analyzed as follows. Each spinal image was printed out in its entirety with no restrictions as to upper or lower count limits. The length of the spine was always parallel to the x-axis of the computer output. For each matrix column parallel to the y-axis, the y channel containing the highest count was marked and thus the maximum count line along the length of the spine was identified. The complete spinal computer output of each patient was divided into six equal rectangular segments which ranged in length from 19 to 21 matrix channels for the patients studied. Figure 1 and Table 2 show the approximate anatomic location of the six spinal segments. For all patients the width of each segment was seven matrix channels, three channels on either side of the maximum count line, thus allowing for spinal curvature or y-directional variation in patient positioning. Because one matrix channel is approximately 0.25 in. (*8*), each of the six spinal segments was about 5 by 1.75 in. For each patient at each time of measurement, a rectangular background segment was chosen of identical dimensions to the spinal segments and laterally displaced from the edge of approximately the third spinal segment by one matrix channel.

The counts in each segment were totaled, corrected for body background, and the net activity in each segment at each time was calculated by comparison with the equivalent counts for the spinal segment standard. Both the patient and the standard images were recorded over the same area of the gamma camera crystal to allow for the variation in response over the detecting area. Since the standard

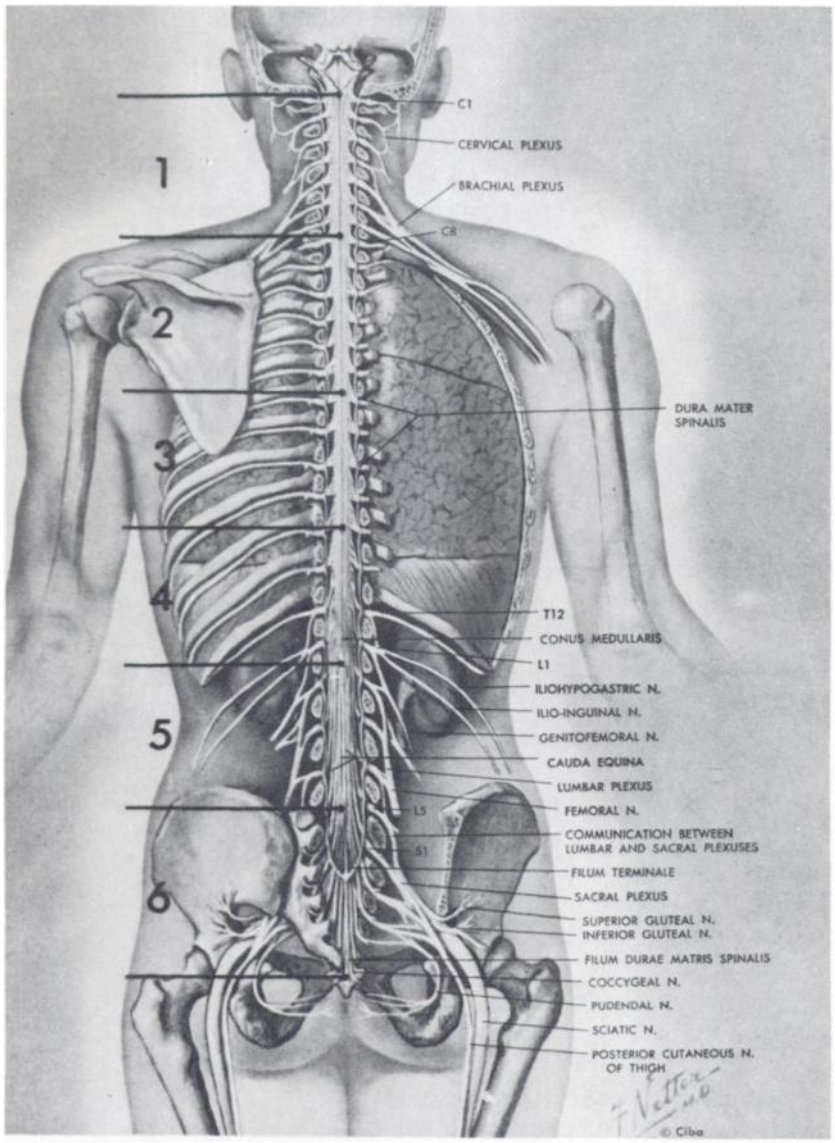

FIG. 1. Anatomic representation of spinal segments 1–6. Adapted, with permission, from Netter FH, *The Ciba collection of Medical Illustrations*. © Copyright 1953, 1972 CIBA Pharmaceutical Co., Div. of Ciba-Geigy Corp. All rights reserved.

was corrected for physical decay of ^{169}Yb from the time of injection to the time of patient measurement, the calculated activity represented the activity remaining as a result of both physical decay and biological clearance of ^{169}Yb-DTPA.

Blood data: collection and analysis. Blood samples were drawn each time patient counting was performed and for three patients (02, 03, and 06, Table 1), additionally up to 96 hr following injection. This was discontinued for subsequent patients since, by 48 hr, blood activity had declined to less than 0.34% of the administered activity. A 1-ml sample from each collection tube was counted with a well counter (Packard Corp., Auto-Gamma Spectrometer) and its activity determined by comparison with the ^{169}Yb sample counting standard.

Tabulated values of total blood volume as a function of height, weight, and sex (*10*) were used to determine each patient's total blood volume, which ranged from 3633 to 5768 ml (mean, 4914 ml). This was then multiplied by the determined activity per milliliter (corrected for decay during the time interval from the time the blood sample was drawn to the time of counting) to obtain the total blood activity remaining in the patient as a result of both physical decay and biological clearance.

RESULTS

Spinal segment activity. For each patient, the ^{169}Yb activity present in each spinal segment at each time counting was performed was plotted as percent of the administered activity as a function of time. Examples of representative activity–time curves for spinal segment 3 are shown in Fig. 2 and include the lowest (Patient 10) and highest (Patient 14) curves for that segment, indicating the typical range

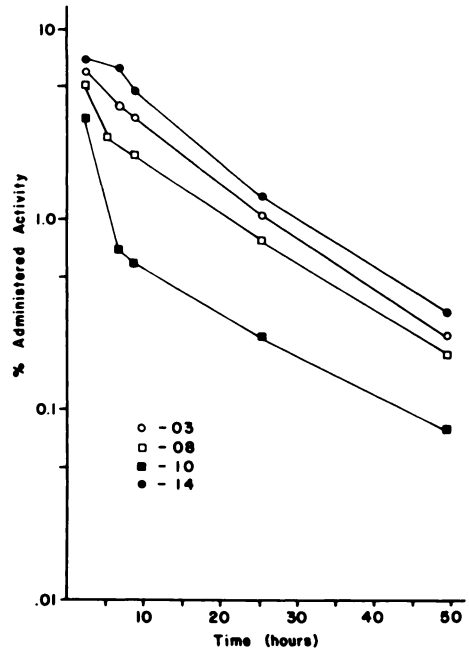

FIG. 2. Examples of activity–time curves for spinal segment 3 (Patients 03, 08, 10, and 14).

TABLE 2. APPROXIMATE ANATOMIC REGIONS OF SPINAL SEGMENTS

Spinal segment	Approximate spinal cord level	Approximate vertebral level
1	C1-C7	C1-C6
2	C8-T6	C7-T5
3	T7-L1	T6-T10
4	L2-Co1	T11-L1
5	Nerve roots	L2-L5
6	Nerve roots	S1-Co1

of patient data. Patients 10 and 14 both had cerebral atrophy and hence delayed flow (Table 1). For all patients studied, the spinal segment activity–time curves could not be divided according to clinical category and hence mean activity–time curves of all patients were obtained for each spinal segment (Fig. 3).

TABLE 3. MEAN CUMULATED ACTIVITY AND PHOTON DOSE ESTIMATES FOR ADMINISTRATION OF 1 mCi ^{169}Yb-DTPA

Segment	$\tilde{A}(\infty)$ (μCi · hr)	$\tilde{A}(t_{eff})$ (μCi · hr)	Mean $\bar{D}_{ph}$ (rads)
1	2922	382	3 ± 2
2	2630	544	4 ± 2
3	3151	715	4 ± 3
4	5376	1457	5 ± 3
5*	6160	2451	8 ± 3
6	4688	1298	5 ± 3

* Includes injection site.

Mean cumulated activities ($\tilde{A}$) were calculated for complete elimination of the radiopharmaceutical by graphic integration of the mean activity–time curves (Fig. 3). Two methods were employed to extrapolate the activity–time curves to infinity. Most conservatively, cumulated activity in each segment was calculated by assuming elimination after the last datum point by solely physical decay [$\tilde{A}(\infty)$] and, least conservatively, also calculated for a final elimination rate equal to that demonstrated at the last datum point [$\tilde{A}(t_{eff})$]; hence, providing a range of values.

$\tilde{A}(\infty)$ values were determined from the graphs using the formula

$$\tilde{A}(\infty) = A_1T_1 + \sum_{j=1}^{n-1}(T_{j+1} - T_j)\left(A_{j+1} + \frac{A_j - A_{j+1}}{2}\right) + 1.44\,A_nT_{1/2}\,e^{\frac{-0.693\,T_n}{T_{1/2}}} \ (\mu Ci \cdot hr) \quad (1)$$

where A_1 is activity (μCi) present at the first observation time T_1 (hr), A_j is activity (μCi) present at the jth observation at time T_j (hr), A_{j+1} is activity (μCi) present at the jth + 1 observation at time T_{j+1} (hr), A_n is activity (μCi) present at the last

TABLE 4. DIMENSIONS OF SPINAL CORD AND SPINAL SUBARACHNOID SPACE*

Spinal segment	Representative vertebra	Spinal cord radii (cm)		Subarachnoid space radii (cm)		CSF volume (cc)
		Frontal	Sagittal	Frontal	Sagittal	
1	C4	0.73	0.44	1.05	0.72	16
2	T2	0.49	0.39	0.73	0.71	12
3	T8	0.41	0.39	0.67	0.75	13
4	T12	0.49	0.48	0.89	0.83	18

* Derived from DiChiro and Fisher (11).

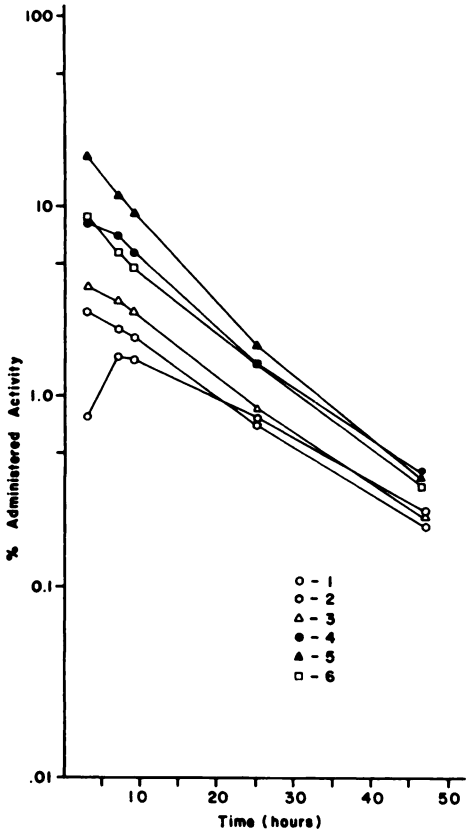

FIG. 3. Mean activity–time curves for spinal segments 1–6.

observation at time T_n (hr), and $T_{1/2}$ is physical half-life (hr). $\tilde{A}(t_{eff})$ values were determined by substituting for $T_{1/2}$, in the last term of Eq. 1, the effective clearance half-time (t_{eff}), which was determined from the slope of the activity–time curve at the time of the last datum point. When the activity–time curve demonstrated an uptake component, the first term in Eq. 1, A_1T_1, was replaced by ½ A_1T_1.

For administration of 1 mCi ^{169}Yb-DTPA, $\tilde{A}(\infty)$ values (Table 3) ranged from 2922 to 4688 μCi·hr for spinal segments 1–6, with a maximum of 6160 μCi·hr in segment 5, which included the injection site. Assuming the alternate elimination pathway, values of $\tilde{A}(t_{eff})$ (Table 3) ranged from 382 to 1298 μCi·hr for segments 1–6, a reduction of about 60 to 90%. The maximum value was 2451 μCi·hr in segment 5. Both these methods of determining cumulated activity are extreme cases and thus represent a minimum-to-maximum range.

Spinal segment volumes. The representative vertebrae for spinal segments 1–4 and their frontal and sagittal dimensions (*11*) are given in Table 4. Spinal fluid volumes for segments 1–4 (Table 4) were calculated assuming concentric cylinders (spinal cord and subarachnoid space) with elliptical cross sections and length 11.7 cm in the crainocaudal direction. According to reported data (*9,12–15*), the most realistic estimate of total spinal CSF volume is 90 ± 15 ml and, therefore, segments 5 and 6 (nerve roots) were each assigned a volume of 15.5 ± 7.5 ml.

Spinal segment dosimetry. Assuming a uniform isotropic model, the general dose equation is (*16*):

$$\bar{D}(v \leftarrow r) = \tilde{A}_r \sum_i \Delta_i \Phi_i(v \longleftrightarrow r)\,(\text{rad}) \qquad (2)$$

where $\bar{D}(v \leftarrow r)$ is average dose-to-target region v from source region r, $\tilde{A}_r$ is cumulated activity (μCi·hr) in source region r, Δ_i is equilibrium dose constant for ith radiation (gm·rad/μCi·hr), and $\Phi_i(v \longleftrightarrow r)$ is specific absorbed fraction for ith radiation (gm^{-1}). Using the reciprocity principle (*16*) the specific absorbed fraction can be expressed as

$$\Phi_i(v \longleftrightarrow r) = [\phi_i(r \leftarrow v)/m_r](gm^{-1}) \qquad (3)$$

where $\phi_i(r \leftarrow v)$ is fraction of energy absorbed in source region r from target volume v and m_r is mass of source region r (gm).

The Δ_i values for the 51 different radiations of ^{169}Yb were obtained through the courtesy of Robert H. Rohrer and are to be published (*7*). For the photons (12 gamma rays and 5 x-rays) resulting from ^{169}Yb decay, $\phi_i(r \leftarrow v)$ values were obtained for each spinal segment assuming a uniformly distributed source in a small 20-gm ellipsoid surrounded by a scattering medium (*17*). The value of $\sum_i \Delta_i \phi_i (r \leftarrow v)$ for photons was 0.0284 gm·rad/μCi·hr. The mean absorbed radiation dose due to photons for 1 mCi administered ranged from 3 to 5 rads for spinal segments 1–6 with a maximum of 8 rads for segment 5 (Table 3).

Ytterbium-169 decay results in 28 internal conversion electrons and 5 Auger electrons, of energies 0.0019–0.3058 MeV (*7*) and ranges in water of 0.17×10^{-4} to 0.083 cm (*18*). The net weighted mean electron energy is 0.013 MeV with a range in water of about 0.0005 cm. In determining the absorbed radiation dose to the cord and nerve roots due to these electrons, usual dosimetry assumptions, namely an infinite, homogenous, unbounded medium, cannot be made because of the source–target geometry of the subarachnoid space and spinal cord and because of the presence of a great many electrons of very low energy with very small ranges in tissue. The spinal cord and nerve roots have radii of about 0.5 and 0.05 cm, respectively, and the surrounding annular cylindrical sheath of spinal fluid an outer radius of about 0.8 cm (*9,11,15*). All the electrons

resulting from the decay of ^{169}Yb in the CSF do not reach the spinal cord and hence absorbed doses due to electron emission would be greatly overestimated if the cord and canal were considered together as one volume with 100% absorption of the electrons. Additionally, because of their very low energy, most of the electrons will be absorbed within a very short distance from the surface of the cord, and, therefore, the absorbed dose from electrons is also dependent upon the depth within the cord.

In order to determine accurately the mean absorbed radiation dose from electrons ($\overline{D}_e$), doses calculated from Eq. 2 ($\phi_i = 1$) must be multiplied by a dose-reduction coefficient C which takes into account the presence of a cylindrical source-free region (the cord or nerve root). C is a function of both the radius of the cylinder and of the depth within it from the surface. Values of C were computed for ^{169}Yb (*19*) from the data of Berger (*18,20*) for radii r = 0.5 cm (cord) and r = 0.05 cm (nerve root) and are plotted in Fig. 4 as a function of the depth within the cord or nerve root. C is a maximum

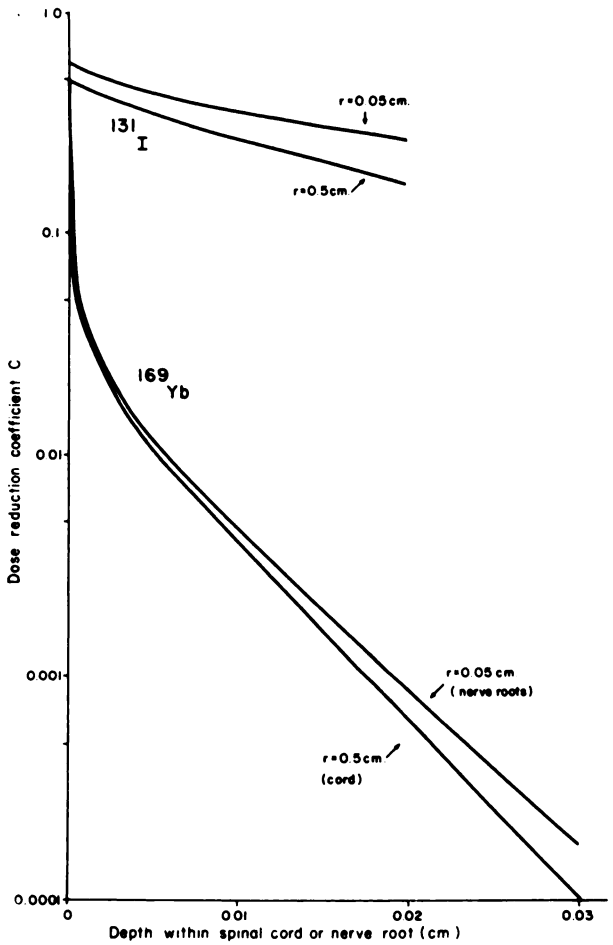

FIG. 4. Dose-reduction coefficient C for electrons of ^{169}Yb and ^{131}I and source-free cylindrical geometry.

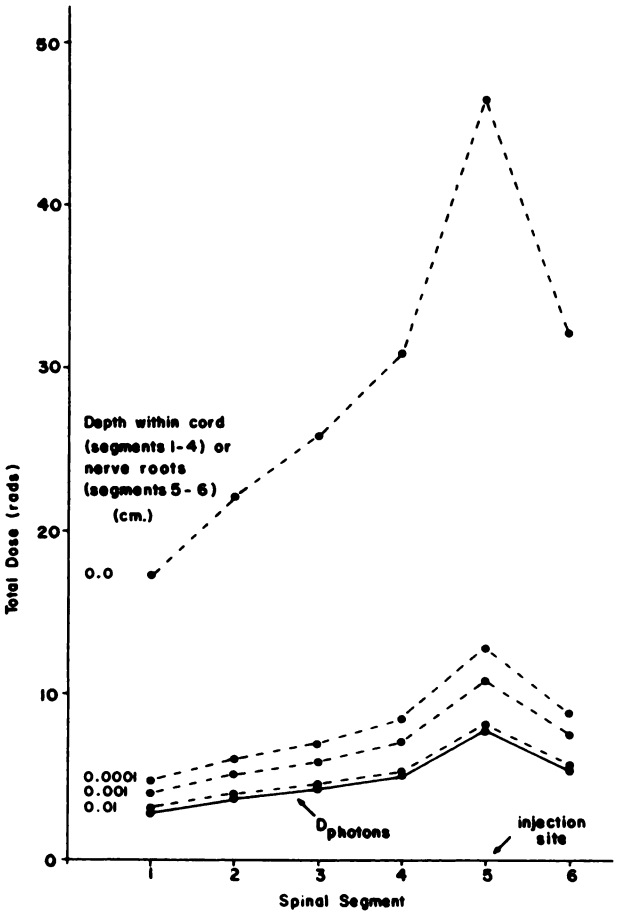

FIG. 5. Mean absorbed dose distribution per millicurie ^{169}Yb-DTPA along length of spine at various depths within spinal cord and nerve roots (see text for discussion of errors).

at the surface (0.5) and decreases very rapidly with distance from the source surface, falling to about 0.063 at 0.0001 cm. This is a reflection of the large contribution to the total energy emitted in ^{169}Yb decay from electrons of energy less than 7 keV and with ranges in tissue less than about 1 micron. Outside this region, the electron-dose-reduction coefficient, and therefore the electron dose, decreases much less rapidly with increasing depth. By 0.001 cm and 0.01 cm [the thickness of the pia (*21*)] from the source surface, C is about 0.038 and 0.004, respectively, and electron doses are 7.5% and 0.9% of the surface doses, respectively. By 0.02-cm depth, C values are only about 0.0007 and therefore the absorbed radiation dose from electrons is about 0.15% of the surface dose.

Also plotted in Fig. 4 are the dose-reduction coefficients for the electrons of ^{131}I, for the same geometry and radii of 0.5 cm and 0.05 cm. At the source surface, these coefficients are about 0.5 and 0.6, respectively. They decrease much more slowly with depth, compared with ^{169}Yb, because of the much

greater mean energy of the electrons, 0.183 MeV with a 90-percentile distance in water of 0.0822 cm (*22*).

For the electrons resulting from ^{169}Yb decay, $\sum_i \Delta_i \phi_i(r \leftarrow v) = 0.278$ gm·rad/μCi·hr. The appropriate value of C was applied to the electron contributions to the absorbed doses calculated from Eq. 2. For segments 1–4 (cord), C values for r = 0.5 cm were employed and for segments 5 and 6 (nerve roots), C values for r = 0.05 cm employed. The mean absorbed doses due to electrons ($\bar{D}_e$) per millicurie of ^{169}Yb-DTPA at the surface ranged from 14 to 27 rads for spinal segments 1–6 with a maximum of 39 rads in segment 5. At a depth of 0.02 cm, $\bar{D}_e$ for segments 1–6 was 0.02–0.05 rads, the maximum dose, 0.07 rads, in segment 5.

The total mean absorbed radiation doses ($\bar{D}_{ph} + \bar{D}_e$) per millicurie of ^{169}Yb-DTPA at various depths from the surface of the cord (segments 1–4) and from the surface of the nerve roots (segments 5 and 6) are given in Fig. 5. Doses are maximal at the surface where $\bar{D}_e$ is five times $\bar{D}_{ph}$. By 0.0001-cm depth, $\bar{D}_e$ is 0.6 $\bar{D}_{ph}$ and by 0.01-cm depth, $\bar{D}_e$ is only 0.04 $\bar{D}_{ph}$. By 0.02-cm depth $\bar{D}_e$ is 0.01 $\bar{D}_{ph}$, less than 0.07 rad for all segments, and therefore negligible compared with $\bar{D}_{ph}$.

Blood activity and dosimetry. Blood activity data were plotted as the percent of administered activity as a function of time and fell into two groups, unrelated to clinical category but related to injection technique. Uptake components were seen for patients 02, 03, and 06 while the remaining four patients indicated instantaneous uptake of ^{169}Yb-DTPA in the blood. Examples are shown in Fig. 6. Because the blood activity–time curves for patients who were known to have unsatisfactory injections were similar to those resembling instantaneous uptake, rapid appearance of ^{169}Yb-DTPA in blood was due to incomplete administration of the radiopharmaceutical into subarachnoid space. Since ^{169}Yb-DTPA is removed from the blood solely by glomerular filtration (*1*), the blood activity–time curve is a function of the glomerular filtration rate and hence a mean activity–time curve was calculated from all patient data for radiation dose estimates for blood.

Mean values of cumulated activity for the administration of 1 mCi ^{169}Yb-DTPA were calculated from Eq. 1 by graphic integration of the mean activity–time curve (Fig. 7). Values of $\tilde{A}(\infty)$ and $\tilde{A}(t_{eff})$ were obtained as for the spinal segment data and were found to be 1005 and 467 μCi·hr, respectively.

Dose estimates were determined from Eq. 2, assuming the blood, with a target mass of 5400 gm, to be uniformly distributed throughout the entire body. For the electrons of ^{169}Yb, the absorbed fraction $\phi_i(v \leftrightarrow v)$ was assumed to be 1 (total absorption). For the photons, values of $\phi_i(v \leftrightarrow v)$ were obtained by assuming source and target to be uniformly distributed throughout the total body (*23*). The values of $\sum_i \Delta_i \phi_i(v \leftrightarrow v)$ were 0.286 for electrons and 0.275 for photons. The total dose estimates ($\bar{D}_t$) to the blood from intrathecal administration of 1 mCi ^{169}Yb-DTPA range from 0.05 to 0.10 rads.

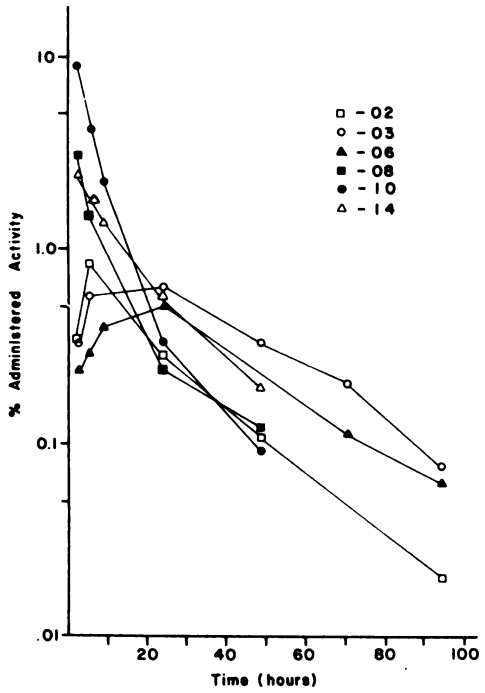

FIG. 6. Examples of blood activity–time curves (Patients 02, 03, 06, 08, 10, and 14).

DISCUSSION

Effective half-times (t_{eff}) for spinal segment clearance of ^{169}Yb-DTPA computed according to the elimination rate at the last datum point of the activity–time curves ranged from 9 to 13 hr. These values are in agreement with the values reported by DeLand (*5*) for the first component spinal segment clearance of ^{169}Yb-DTPA in dogs, ranging from about 12 to 13 hr. In addition, DeLand (*5*) reported a delayed clearance component of approximately 13 to 14 days. As we were not able to obtain patient data beyond 48 hr due to surgery and/or discharge from the hospital, the delayed clearance component was not demonstrated in the present study. However, we have considered elimination beyond 48 hr by solely physical decay (the most conservative estimate) and at the rate demonstrated at the last datum point, hence establishing a range.

The ranges given for the dose estimates in Tables 3, 5, and 6 reflect the two methods of extrapolating the clearance data (Figs. 3 and 7) to infinity. There is, however, additional uncertainty in the dose estimates for segments 5 and 6 due to the uncertainty of ±7.5 ml in the assigned spinal fluid volumes of 15.5 ml (See Results section). Hence all the dose estimates for segments 5 and 6 in Fig. 5 and Tables 3 and 6 may be additionally higher or lower by a factor of 1.9 or 0.7, respectively.

Because all patients in this investigation demonstrated slow cisternographic clearance, the cumulated activities and hence the dose estimates are higher than would be expected for cisternography in the normal individual.

As was evidenced by the blood clearance curves (Fig. 6), not all the ^{169}Yb-DTPA was deposited in subarachnoid space. Although the general shape of the spinal segment activity–time curves appeared to be similar for all patients studied, a variation was observed in the y-placement of the curves (Fig. 2), unrelated to clinical category. Because the activity injected into each patient had been precisely determined, the variation in the distribution of the curves was attributed to variation in the quality of the injection and hence to variation in the amount of the administered activity injected into the subarachnoid space. Deposition of the radiopharmaceutical into other than subarachnoid space (subdural or epidural space) results in a misstatement of the injected activity and affects the calculated percent of administered activity present. Since some portion of the injected activity remains in the spinal subarachnoid space, the cisternogram can be clinically evaluated. However, quantitative determinations are inaccurate by a factor which is related to the technical quality of the injection. This clinical problem has been previously stated (*15,24–27*) and has been reported to occur is as many as 27% of the cases studied (*25*). Intrathecal administration of 100 μCi ^{131}I-IHSA gives a mean radiation dose to the blood of 0.5 rads (*15*) which is at least five times the values for 1 mCi ^{169}Yb-DTPA.

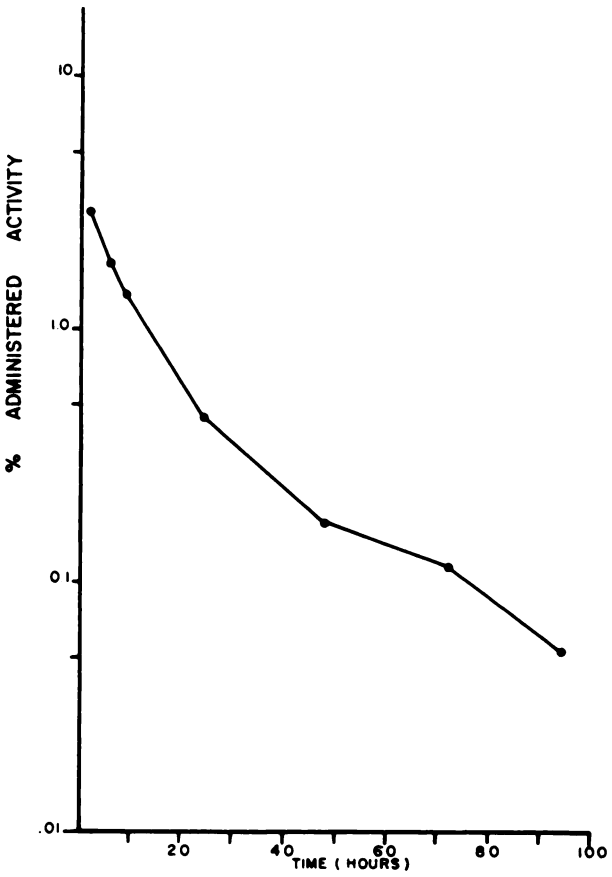

FIG. 7. Mean activity–time curve for blood.

The spinal segment activity–time curves obtained utilizing ^{169}Yb-DTPA (Fig. 2) are similar in shape to those obtained with ^{131}I-IHSA (*9,28*), thus indicating the reported similarity in the biological behavior of both radiopharmaceuticals within the CSF (*29*). Considerable attention has been given to the absorbed radiation dose to the spinal cord during cisternography utilizing ^{131}I-IHSA (*9,15,21,30–34*) with reported dose estimates ranging from 1 rad (*31*) to 600 rads (*32*) following intrathecal injection of 100 μCi ^{131}I-IHSA. This variation in dose estimates arises from the various assumptions made in determining the CSF volume and the cumulated activity in the subarachnoid space and in the treatment of the spinal cord source–target geometry.

The most realistic estimates of the absorbed dose to the spinal cord and nerve roots in ^{131}I-IHSA cisternography have been obtained by Johnston, et al (*15*) and Harbert, et al (*9*). They utilized electron-dose-reduction coefficients for ^{131}I and appropriate cylindrical geometry. Tables 5 and 6 summarize dose estimates to the cord and nerve roots, respectively, for 1 mCi ^{169}Yb-DTPA and 100 μCi ^{131}I-IHSA. For ^{169}Yb-DTPA, the cord and nerve root dose estimates tabulated are for segments 4 and 5, respectively, since they represent the highest doses to cord and nerve roots. Johnston, et al (*15*) found no significant differences between the ^{131}I-IHSA cisternographic data for their 12 patients and, like this report, considered all patients together in one sample. Harbert, et al (*9*) considered separately nine patients with normal clearance, four with hydrocephalus, and one with cervical block. The dose estimates extracted from their report (*9*) and given in Tables 5 and 6 represent the total ranges for all their patients and

TABLE 5. COMPARATIVE ABSORBED DOSES (RADS) TO CORD FROM INTRATHECALLY ADMINISTERED ^{169}Yb-DTPA AND ^{131}I-IHSA

Depth (cm)		0	0.0001	0.001	0.01	0.02
^{169}Yb-DTPA (1 mCi)	Range	13–49	4–13	3–11	2–9	2–8
	Mean	31	8	7	5	5
^{131}I-IHSA (100 μCi)	*Range	12–27		11–25	7–15	5–10
	*Mean	16		14	9	6
	†Range	7–59			4–33	2–19
	†Mean	12			7	4

* (15).
† (9).

TABLE 6. COMPARATIVE ABSORBED DOSES (RADS) TO NERVE ROOTS FROM INTRATHECALLY ADMINISTERED ^{169}Yb-DTPA AND ^{131}I-IHSA

Depth within nerve root (cm)		0	0.0001	0.001	0.01	0.02
^{169}Yb-DTPA (1 mCi)	Range	26–66	7–18	6–15	5–12	5–11
	Mean	46	13	11	8	8
^{131}I-IHSA (100 μCi)	*Range	13–33		12–29	9–20	7–15
	*Mean	19		17	12	9
	†Range	8–76			6–46	5–39
	†Mean	15			10	8

* (15).
† (9).

net weighted means for 10-ml segmental volumes (higher dose estimate).

Because the quoted thickness of the pia [0.01 cm (*21*)] is only an order of magnitude, no precise delineation is made between "pia dose" and "cord dose". Hence the spinal cord absorbed radiation doses are presented, most generally, in Fig. 5 and Table 5 as a function of total depth from the surface including the thickness of the pia.

The absorbed doses from 1 mCi of ^{169}Yb-DTPA are two and one-half times those from 100 μCi ^{131}I-IHSA at the surface, but, as expected from the electron dose-reduction coefficients plotted in Fig. 4, decrease much more rapidly with depth. By 0.01-cm depth, the average absorbed doses are due solely to the photons from ^{169}Yb (see Table 3 and Fig. 5). The cord and nerve root absorbed doses from ^{131}I-IHSA decrease much more slowly with depth, eventually reaching the values of about 0.1 rad (*9*) to 1.5 rad (*15*) due solely to the photons from ^{131}I.

The average total absorbed dose is the sum of the average electron dose integrated throughout the cord or nerve root and the photon dose. For ^{169}Yb-DTPA the average electron doses throughout the cord and nerve roots are only about 0.1% and 1%, respectively, of the surface doses and hence, the average total doses are the photon doses, about 5 and 8 rads, respectively, for 1 mCi (Table 3 and Fig. 5). For ^{131}I-IHSA, the average electron dose to the cord has been estimated to be one-ninth of the surface dose (*21*) and for 100 μCi is, therefore, about 1.4 rads (from the data in Table 5). Hence the average total dose throughout the cord is about 1.5 to 2.9 rads, which is about 0.4 that of the equivalent value from 1 mCi ^{169}Yb-DTPA.

A recent clinical study (*29*) of the cisternographic patterns and CSF clearance in 12 patients with suspected hydrocephalus concluded that, for most cisternography, ^{169}Yb-DTPA is a superior tracer compared with ^{131}I-IHSA. Advantages of ^{169}Yb-DTPA over ^{131}I-IHSA as a cisternographic agent include the following: there is no risk of potential toxicity of albumin and its contamination with bacterial endotoxin (*35*); no thyroid blocking is required; the lower-energy gamma rays are more easily collimated; the longer physical half-life results in a longer shelf-

life of the radiopharmaceutical and enables higher-quality images to be recorded at greater times after administration. This report indicates that surface and average absorbed radiation doses to spinal cord and nerve roots from 0.4 mCi ^{169}Yb-DTPA and 100 μCi ^{131}I-IHSA are approximately equal or, stated alternatively, for equal administered dose, ^{169}Yb-DTPA, a gamma-ray emitter, gives one-fourth the absorbed radiation dose to spinal cord and nerve root as does ^{131}I-IHSA, a beta- and gamma-ray emitter. The abundance of the useful 364-keV gamma ray of ^{131}I is 0.833/disintegration (*36*) and is one and one-half times the combined abundance, 0.553/disintegration, of the useful 177- and 198-keV gamma rays of ^{169}Yb (*7*). Hence, assuming other things equal, the photon flux from 400 μCi ^{169}Yb-DTPA is greater than that from 100 μCi ^{131}I-IHSA by a factor of 2.7 and, therefore, image quality is better for the same absorbed radiation doses to cord and nerve roots. We conclude that ^{169}Yb-DTPA is superior to ^{131}I-IHSA as a cisternographic agent.

ACKNOWLEDGMENTS

The authors thank Lawrence T. Fitzgerald and Martin J. Berger for assistance in the determination of electron dose-reduction coefficients, Clyde M. Williams and Frank H. DeLand for helpful discussion and advice, and Marshall L. Sunderland for technical assistance. This work was supported in part by USPHS Training Grant RL00047-10 and was presented at the 14th annual meeting of the Southeastern Chapter of the Society of Nuclear Medicine.

REFERENCES

1. HOSAIN F, REBA RC, WAGNER HN: Measurement of glomerular filtration rate using chelated ytterbium-169. *Int J Appl Radiat Isot* 20: 517–521, 1969

2. WAGNER HN, HOSAIN F, DELAND FH, et al: A new radiopharmaceutical for cisternography-chelated ytterbium-169. *Radiology* 95: 121–125, 1970

3. JAMES AE, HOSAIN F, DELAND FH, et al: ^{169}Ytterbium diethylenetriaminepentaacetic acid (^{169}Yb-DTPA)—a versatile radiopharmaceutical. *J Can Assoc Radiol* 22: 136–143, 1971

4. DELAND FH, JAMES AE, WAGNER HN, et al: Cisternography with ^{169}Yb-DTPA. *J Nucl Med* 12: 683–689, 1971

5. DELAND FH: Biological behavior of ^{169}Yb-DTPA after intrathecal administration. *J Nucl Med* 14: 93–98, 1973

6. HARBERT JC: Radionuclide Cisternography. *Semin Nucl Med* 1: 90–106, 1971

7. DILLMAN LT, VON DER LAGE FC: Radionuclide decay schemes and nuclear parameters for use in radiation dose estimation. MIRD Pamphlet No 10, *J Nucl Med*, 1974

8. BRUNO FP, BROOKEMAN VA, WILLIAMS CM: A digital computer data acquisition, display, and analysis system for the gamma camera. *Radiology* 96: 658–661, 1970

9. HARBERT JC, MCCULLOUGH DC, ZEIGER LS, et al: Spinal cord dosimetry in ^{131}I-IHSA cisternography. *J Nucl Med* 11: 534–541, 1970

10. NADLER SB, HIDALGO JU, BLOCH T: Prediction of blood volume in normal human adults. *Surgery* 51: 224–232, 1962

11. DICHIRO G, FISHER RL: Contrast radiography of the spinal cord. *Arch Neurol* 11: 125–143, 1964

12. LINDGREN E: Myelographie mit luft. *Nervenarzt* 12: 57–61, 1939

13. LUPS S, HAAN AMFH: *The Cerebrospinal Fluid.* Amsterdam, Elsevier, 1954, p 15

14. BULL J: Radiation dose in isotope encephalography. *Lancet* 1: 357–358, 1968

15. JOHNSTON RE, STAAB EV, BRILL AB, et al: Radiation dosimetry associated with intrathecal administration of ^{131}I human serum albumin. *Br J Radiol* 45: 444–451, 1972

16. LOEVINGER R, BERMAN M: A schema for absorbed-dose calculations for biologically distributed radionuclides. MIRD Pamphlet No 1, *J Nucl Med* 9: Suppl No 1, 7–14, 1968

17. ELLETT WH, HUMES RM: Absorbed fractions for small volumes containing photon-emitting radioactivity. MIRD Pamphlet No 8, *J Nucl Med* 12: Suppl No 5, 25–32, 1971

18. BERGER MJ: Improved point kernels for electron and beta-ray dosimetry. Washington, NBS, #NBSIR 73-107, 1973

19. BROOKEMAN VA, FITZGERALD LT, MORIN RL: to be published

20. BERGER MJ: Beta-ray dosimetry calculations with the use of point kernels. In *Medical Radionuclides—Radiation Dose and Effects,* Oak Ridge, USAEC, CONF-691212, 1970, pp 63–86

21. HILDITCH TE: Radiation dose in isotope encephalography. *Lancet* 2: 573–574, 1968

22. BERGER MJ: Distribution of absorbed dose around point sources of electrons and beta particles in water and other media. MIRD Pamphlet No 7, *J Nucl Med* 12: Suppl No 5, 5–23, 1971

23. SNYDER WS, FORD MR, WARNER GG, et al: Estimates of absorbed fractions for monoenergetic photon sources uniformly distributed in various organs of a heterogeneous phantom. MIRD Pamphlet No 5, *J Nucl Med* 10: Suppl No 3, 5–52, 1969

24. KIEFFER SA, WOLFF JM, PRENTICE WB, et al: Scinticisternography in individuals without known neurological disease. *Am J Roentgenol Radium Ther Nucl Med* 112: 225–236, 1971

25. SANDERS TP, SANDERS TD, GALLAGHER EJ: Quantitative studies of CSF dynamics. In *Cisternography and Hydrocephalus,* Springfield, Ill, CC Thomas, 1972, pp 463–470

26. LARSON SM, SCHALL GL, DICHIRO G: The influence of previous lumbar puncture and pneumoencephalography on the incidence of unsuccessful radioisotope cisternography. *J Nucl Med* 12: 555–557, 1971

27. CURL FD, HARBERT JC, MCCULLOUGH DC: Quantitative cisternography—an aid to diagnosis. In *Cisternography and Hydrocephalus,* Springfield, II, CC Thomas, 1972, pp 441–451

28. CHOU SN, FRENCH LA: Systemic absorption and urinary excretion of RISA from subarachnoid space. *Neurology* 5: 555–557, 1955

29. HARBERT JC, REED V, MCCULLOUGH DC: Comparison between ^{131}I-IHSA and ^{169}Yb-DTPA for cisternography. *J Nucl Med* 14: 765–768, 1973

30. HÜBNER KF, BROWN DW: Scanning of the spinal subarachnoid space after intrathecal injection of ^{131}I labeled human serum albumin. *J Nucl Med* 6: 465–472, 1965

31. BANNISTER R, GILFORD E, KOCEN R: Isotope encephalography in the diagnosis of dementia due to communicating hydrocephalus. *Lancet* 2: 1014–1017, 1967

32. SEAR R, COHEN M: Radiation dose in isotope encephalography. *Lancet* 1: 249, 1968

33. BROCKLEHURST G: Radiation dose in isotope encephalography. *Lancet* 1: 358, 1968

34. MCALISTER JM: Radiation dose in isotope encephalography. *Lancet* 1: 526–527, 1968

35. HOSAIN F, SOM P, JAMES AE, et al: Radioactive chelates for cisternography—the basis and the choice. In *Cisternography and Hydrocephalus*, Springfield, Ill, CC Thomas, 1972, pp 185–193

36. DILLMAN LT: Radionuclide decay schemes and nuclear parameters for use in radiation-dose estimation. MIRD Pamphlet No 4, *J Nucl Med* 10: Suppl No 2, 5–32, 1969